Molecular Weight and Secondary Structure Change in Eri Silk During Alkali Degumming and Powdering

Rangam Rajkhowa,[1] Lijing Wang,[2] Jagat R. Kanwar,[1] Xungai Wang[1]

[1]*Institute for Technology Research and Innovation, Deakin University, Geelong, VIC 3217, Australia*
[2]*School of Fashion and Textiles, RMIT University, Brunswick, VIC 3056, Australia*

Received 1 March 2009; accepted 15 December 2009
DOI 10.1002/app.31981
Published online 18 August 2010 in Wiley Online Library (wileyonlinelibrary.com).

ABSTRACT: Changes in molecular weight and secondary structure of eri silk during alkali degumming and silk powdering were studied. An increase in silk degumming intensity, through increased alkali concentration, treatment temperature, and time, reduced the fibroin molecular weight and, therefore, the fiber tenacity, but at the same time, increased the β-sheet fraction. These changes reduced the time required to mill the degummed silk fibers into fine powders. Mechanical forces used in wet attritor and air jet milling disturbed intermolecular packing along the direction of side chains, but the conformation remained essentially β-sheet even in the sub-micron silk particles. Dry milling drastically reduced molecular weight and changed the conformation of the fibroin chains. The rate of the spontaneous conformation transition in regenerated fibroin solution prepared from fibers and powders increased with a decrease in fibroin molecular weight, affecting the time fibroin solutions could be stored before gelling. Overall, the study showed that molecular weight and secondary structure of silk powders could be manipulated by suitably changing the degumming and milling conditions. It also suggests that wet media milling and air jet milling are better than dry media milling to prepare less degraded and more crystalline ultrafine silk particles. © 2010 Wiley Periodicals, Inc. J Appl Polym Sci 119: 1339–1347, 2011

Key words: biopolymers; gelation; microstructure; silk; particles

INTRODUCTION

Silkworm silk and spider silk are well-suited for use as advanced biomaterials due to their good mechanical properties, biocompatibility, and slow resorption times.[1–6] In most applications, silk is usually regenerated into various forms, such as nonwovens,[7] nano fiber matts,[4,8] films,[4] hydrogels,[9–11] foams,[4,12] and powders.[2,13–17] These regenerated forms usually have inadequate properties for some applications and are soluble in water until β-sheets are formed by treatment with methanol and other solvents, but such solvent treated products are often brittle.[18]

Powders produced by mechanically milled silk fibers provide an alternative form of silk biomaterial. This avoids long processing time and harmful chemicals used in solution routes. However, milling viscoelastic silk fibers to fabricate fine particles has been a challenge. Taking advantage of the inherent multilevel nano-fibrillar structure of silk fibers, we have recently optimized silk milling process to prepare sub-micron particles.[19,20] The advancement in milling may boost existing applications of silk powder, such as in cosmetics. We have also identified the potential of these particles for reversible binding of heavy metal ions[21] and use in composite scaffolds for tissue engineering.[22] In addition, the particles may find other advanced biological applications, as lack of ultrafine particles with desired morphology was suggested to be responsible for application limitations of milled silk powder.[23] Regenerated silk powders have been studied for wound care,[2] enzyme immobilization,[13–15] and drug delivery[16,17] applications.

To date, no systematic examination on effects of various milling parameters on microstructure of silk has been reported, though milling effects on reduction in molecular weight and crystallinity of synthetic and other natural polymer powders have been examined.[24–26] This study is designed to reveal whether the powdering process causes relative conformational changes in β-sheet dominated structure of silk fibers. The role of alkali degumming on silk microstructure has also been included as it plays an important role in milling efficiency, particle size, and particle morphology.[19] So far, the effect of degumming conditions on secondary structure of silk has not been examined although degradation of silk during degumming was reported.[27–31]

Understanding changes in microstructure during processing of silk fibroin is important because it has important influence on functional properties of silk materials. For instance, Tsubouchi et al. reported

Correspondence to: X. Wang (xwang@deakin.edu.au).

that reduction in molecular weight during degumming reduced the bioactivity of silk to support cells.[32] Similarly, the release of drugs and enzymes can be accelerated with the reduction of β-sheet in silk.[16,33–35] Furthermore, it was shown that lower β-sheet content accelerated biodegradation rate of silk products.[36,37] On the other hand, high molecular weight and β-sheet content in silk fibroin are desired for greater stability and mechanical properties. In case of particles, these may be particularly helpful for some applications, such as reinforcement and as scavenger for ion separation. Thus, the structural information will be useful to optimize processing methods to suit end applications of silk powder. Furthermore, such information may open new application opportunities.

This study focuses on eri silk from *Philosomia cynthia ricini* (*P. c. ricini*), also known as *Samia cynthia ricini*, silkworms that belong to the Saturniid family. The eri silk milling is more efficient than milling of the well-known mulberry silk from *Bombyx mori* (*B. mori*).[19,20] Eri silkworms also have advantages over other non-mulberry silkworm species due to widely available host plant, better disease resistance, and in house rearing, which make eri silk a potential source for making silk powder.

EXPERIMENTAL

Material preparation

Raw cocoons of indoor reared eri silk of *P. c. ricini* silkworm and mulberry silk of *B. mori* silkworm were purchased from silk cocoon production centers in Northeast India.

Degumming

The cocoons were degummed before milling to remove the sericin present in fibroin protein. Mostly, degumming was performed according to the conditions normally used in the eri spun silk industry, which is adequate to remove the gum. This is referred to as "normal degumming" in this work. Before milling, it is a common practice to use pretreatments (e.g., alkali, acid, radiation, or steam explosion), which substantially reduce fiber strength to improve milling efficiency.[38–41] Harsher alkaline degumming conditions than that commonly used for commercial silk degumming were used to reduce fiber strength in this work. Such a degumming treatment is referred to as "intensive degumming" in this article. In addition, a smaller batch of eri silk fibers was degummed under milder degumming conditions than that used for "normal degumming to use as a control during molecular weight measurements. To ensure minimum fiber degradation and effective gum removal, this degumming process was performed for a short period with multiple repeats. This is referred to as "control degumming." The following specific degumming conditions were used for each method.

Normal degumming. Eri cocoons of 1 kg per batch were degummed with a laboratory dyeing machine (from Thies) using laboratory grade 2 g/L sodium carbonate and 0.6 g/L sodium dodecyl sulfate (from Sigma Aldrich) at 100°C with a material (kg) to liquor (L) ratio of 1 : 25. After degumming, the cocoons were thoroughly washed with warm distilled water followed by cold distilled water. For a comparative study of molecular weight, cocoons of *B. mori* silk were also degummed using the same procedure. Preliminary experiments were performed on weight loss during degumming by changing treatment time to confirm that sericin was removed. Treatment times of 120 and 20 min were found ideal to reach maximum weight loss of 14–15% and 29–30% for eri and mulberry silk, respectively, and hence, different normal degumming times for the two silk varieties were used in this study.

Intensive degumming. Concentration of sodium carbonate was increased to 10 g/L and temperature to 120°C. Material to liquor ratio was reduced to 1 : 10. Other processing parameters were the same as for eri silk normal degumming.

Control degumming. The cocoons were degummed with a laboratory dyeing machine (Ahiba Nuance) in small lots of 10 g, using laboratory grade 1 g/L sodium bicarbonate and 0.6 g/L sodium dodecyl sulfate (from Sigma Aldrich) at 100°C with a fiber mass (g) to liquor volume (mL) ratio of 1 : 50 for 30 min. This was repeated thrice. The cocoons were then thoroughly washed with warm distilled water followed by cold distilled water.

Powder preparation

The details of powder production were reported in an earlier publication.[19] Briefly, degummed silk fibers were chopped into snippets using a cutter mill (Pulverisette 19 from Fritsch). A stirred ball mill (1S Attritor from Union Process) was used for both dry and wet grinding of the chopped silk fiber snippets using 20 kg yttrium treated zirconium oxide grinding media (5 mm) in a 9.5 L tank. The stirrer speed was 280 rpm. Time of milling was up to 12 h. Distilled water was used in wet grinding operation. Dry powders from wet milled slurry were recovered using a laboratory spray dryer (B-290 from Buchi Labortechnik AG). The inlet temperature and slurry flow rate were 120–140°C and 7–8 mL/min, respectively.

A Sturtevant laboratory air jet mill with an air pressure of 110 kg/cm^2 was also used in the final

step in powder production. Preprocessed silk powder was fed with a powder hopper (K-Tron, made in USA) at a feed rate of 200 g/h and processed continuously by the air jet mill.

Preparation of regenerated silk films

Fiber and powder samples were dissolved in 10*M* lithium thiocyanate at room temperature with a material to liquor ratio of 1 (g) : 10 (mL). Any undissolved parts in the solution were removed using a centrifuge (CT15 RT from Techcomp), operating at 4000 rpm under room temperature for 10 min. The clear solutions were dialyzed for 4 days at 4°C against Mili-Q water using dialysis sacks (molecular weight CO 12,000 Da, Sigma Aldrich). Water was changed every 6–12 h. The final concentration of the silk solutions varied between 2% and 4% (w/v). The actual concentration was determined by weighing the remaining solid after drying overnight at 60°C. The concentration of silk aqueous solution was adjusted by diluting with Mili-Q water to 1% (w/v). The solution was then poured into polyethylene disks and dried at 4°C until dry films were obtained.

Aging regenerated silk

To study the effect of storage time on conformational transition, silk aqueous solutions (concentration adjusted to 1%) were stored for different times up to 3 weeks at 20°C ± 2°C and 65% ± 2% relative humidity and the time to change a transparent solution into a milky form was recorded. The solutions at different time points were poured into polyethylene disks to cast films at 4°C.

Material Characterization

FTIR analysis

Infrared spectra of silk fibers, particles, and films were recorded with an attenuated total reflectance (ATR) Fourier transform infrared (FTIR) spectrophotometer (Vertex 70 from Bruker). Each spectrum was obtained in absorbance mode in the range of 4000–600 cm^{-1}.

X-ray scattering analysis

Wide angle X-ray scattering (WAXS) was performed on a diffractometer (Phillips PW 1729) with Cu Kα radiation ($\lambda = 0.154$ nm), operated at 35 kV and 28 mA. Scanning rate was 0.04°/s. Spectra from different forms of silk materials were analyzed using the TracesV6 software.

In case of silk fibers, specimens for FTIR and XAXS studies were prepared by cutting the fibers into 2 mm snippets using a guillotine. All samples were desiccated before tests.

SDS-PAGE

Aqueous silk solutions were prepared according to the method described in Section ''Preparation of regenerated silk films''. However, the dialysis time was reduced to 6 h only and water was changed every 2 h because solutions from powders and intensively degummed fibers formed gels during long hours of dialysis. Molecular weight was measured with SDS-PAGE without any reducing agent, using 4–20% gradient gels and sample buffer (NH11-420 and BG-165 from Nu Sep), Tris-HEPES-SDS running buffer and molecular weight standards (161-0317 from BioRad) following manufacturers recommended standard protocols. A total of 50 μL of 1% (w/v) silk solutions as determined by weighing the solid after drying were used in each well. Gels were stained with Commassie Blue R-250 (from Sigma Aldrich).

Measurement of fibre tenacity

Single fiber tenacity was measured with a Single Fibre Analyser (SIFAN from BSC Electronics) using a jaw separation speed of 500 mm/min and a gage length of 25 mm. The tested fibers were sampled from the middle layers of degummed cocoons. The fibers were conditioned at 20°C ± 2°C and 65% ± 2% relative humidity for at least 48 h before testing. Their linear density, in dtex or gram per 10,000 meters, was calculated from the scanning electron microscope (LEO 1530 FEG-SEM) measured mean cross-sectional area of cut filaments ($n = 30$) collected from the same cocoon layers used for tensile tests. The density of eri silk (1.314 g/cm^3) was used from our earlier study.[42] This was done as eri fibers could not be reeled out continuously for measurement of linear density by weighing a given length of fiber. Fiber tenacity was calculated from the fiber breaking load and the linear density. A total of 100 silk fibers were tested from each degummed batch.

RESULTS AND DISCUSSION

Molecular weight at different powder processing stages

It is expected that silk fibroins with high Alanine and Glycine contents in heavy chains should show some migration on SDS-PAGE gels compared with normal globular proteins. However, SDS-PAGE can be useful to reveal qualitative changes in molecular weight during powder processing. Figure 1 shows the SDS-PAGE results after different degumming

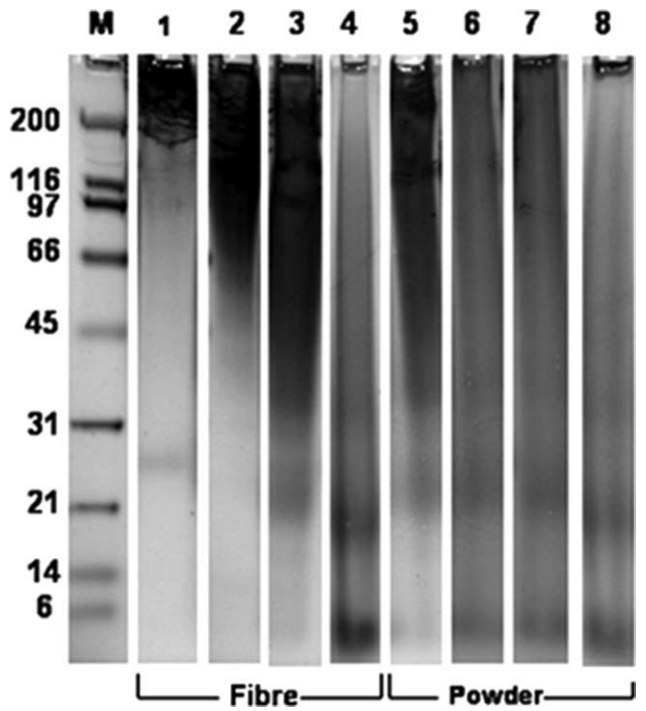

Figure 1 SDS-PAGE of silk fibers (lanes 1–4) and powders milled from normal degummed fiber (lanes 5–8). M, molecular weight standards; lane 1, *B. mori* silk (normal degumming); lanes 2–8, *P. c. ricini* (eri) silk (2, control degumming; 3, normal degumming; 4, intensive degumming; 5, 3 h wet milled; 6, 12 h wet milled; 7, 12 h wet milled + air jet milled; 8, 6 h dry milled).

regimes and at different stages of powder production.

The electrophoretic pattern for the control degummed eri silk fibroin in lane 2 appears to show a molecular weight range from around 60 kD to more than 200 kD. Eri silk is reported to have a homodimeric protein in silkworm's gland, with a molecular weight of ~ 330 kD, formed by individual protein of ~ 160 kD.[43] It is possible that during degumming the individual proteins in the homodimer separate. However, the presence of a smeared pattern, instead of 330 or 160 kD bands, suggests some degradation during degumming. It has been reported that fibroins from domestic *B. mori* and wild *Antheraea pernyi* silk fibers showed greatly smeared bands on SDS-PAGE.[28–30] The degradation was mostly attributed to alkali hydrolysis and, to some extent, the fiber dissolution process.[28,29] To avoid reduction of molecular weight during dissolution, in the present study, Lithium thiocyanate (LiSCN) at ambient temperature was used to prepare fibroin solution. Past studies on *B. mori* silk revealed its superiority compared to other chaotropic solvents.[28] It also emerged as the most effective solvent in dissolving wild silk fibers using a temperature of 40°C or more, where other solvents mostly failed.[29] As LiSCN dissolution was used at room temperature, there was much less smearing in *B. mori* silk as shown in lane 1. Interestingly, a ~ 25 kD band, which is probably the light chain, appears in lane 1, in spite of the absence of reducing agent, suggesting that the light chains were separated from the heavy chains during degumming. Results of lanes 1 and 2 indicate that the time for mild control degumming of eri silk was still long enough (90 min) to cause molecular chain rupture, resulting in a higher level of smearing compared to *B. mori*, which was degummed for less time (20 min). In the case of normal degummed eri silk (lane 3), the smearing is greater compared to control degummed eri (lane 2). Intensively degummed material was highly degraded according to the pattern shown in lane 4, indicating that aggressive alkaline conditions hydrolyzed fibroin molecules substantially. The presence of a broad band below 6 kD mark in the lane 4 possibly indicates that the dialysis membrane could retain some short chains during the short dialysis time. If dialysis continued, either the solution probably gelled or short chains were dialyzed out and as a result, no bands appeared in SDS-PAGE for the degraded samples (result no shown).

To check whether the spray drying process caused any degradation, preliminary tests were conducted for selected samples after milling. Slurry was dried at room temperature before preparing silk solution. The results suggested no change in SDS-PAGE patterns due to spray drying using inlet temperatures within 120–140°C (patterns not included). Measurement of color index as reported previously[19] also suggested no yellowing of wet milled spray dried powder. As drying is very quick and the evaporation leads to a cooling of the droplet and thus low thermal load, the fibroin did not experience noticeable thermal degradation. The spray drying inlet temperature of 120°C was, therefore, used for the samples analyzed in this work. Hence, the degradation showed up in Figure 1 for powders is attributed to milling conditions only. When comparing lane 3 with lane 5, there appears to be no substantial difference between the patterns. However, due to large smearing, it is difficult to differentiate the molecular weight distributions between fiber (lane 3) and 3 h milled powder (lane 5). After 12 h milling, the broad electrophoresis band (lane 6) becomes lighter compared with lane 5, indicating some additional degradation between 3 and 12 h of milling. Subsequent air jet milling after attritor milling did not cause further change in the pattern according to lanes 6 and 7. In the case of dry milled powder (lane 8), the sharpness of the large smeared band has been reduced compared with that of wet milled powders (lanes 6 and 7). It was observed that after 6 h dry milling, there was a distinct change in powder color from white to

TABLE I
Tenacity of Degummed Eri Silk Fibers
(Mean ± SD; n = 100)

Type of degumming	Tenacity (cN/dtex)
Control	4.5 (0.58) ± 1.2
Normal	3.6 (0.46) ± 0.6
Intensive	0.8 (0.10) ± 0.5

Data in parenthesis indicate mean tenacity in GPa.

yellow. This gives an indication of strong degradation during dry milling. A sharp fall in molecular weight of semicrystalline polymers was reported due to complex forces of shearing, fracture, extension and cold welding during high energy dry milling.[44] The results of this study suggest that dry milling method degrades silk faster than the wet milling method. SDS-PAGE results in lanes 3, 5, and 6 demonstrate that degradation can be controlled unless milling continues for too long. Although retaining higher molecular weight distribution in silk powder could be explored by suitably altering the milling parameters, the best approach will be to retain as much of the molecular weight as possible during degumming.

Tensile strength

The milling efficiency of silk is very much dependent on fiber tenacity.[19] Table I shows that the fiber tenacity dropped significantly after intensive degumming. This is because the molecular weight of intensively degummed fibers was drastically reduced. Although there was also an appreciable fall in molecular weight on the normal degummed fibers as shown in Figure 1, the fibers still retained good strength.

Change in secondary structure during degumming and powder production

FTIR is an established technique to study the conformation of proteins, but FTIR studies on eri silk are rare. We have selected characteristic peak maxima for different conformations of eri silk depending on reports of $(Ala)_n$ based other Saturniid family silk materials.[29,30,45–51] Accordingly, peak maxima at 1628 cm^{-1} (amide I, C=O stretching), 1520 cm^{-1} (amide II, N—H bending), 1240 cm^{-1} with shoulders at 1222 cm^{-1} (amide III, C—N stretching), 700 cm^{-1} (amide V, C—N torsion and N—H bending), and at 966 cm^{-1} (skeletal vibration due to Ala-Ala) are attributed to β-sheet. On the other hand, peaks at 1653 cm^{-1} (amide I), 1541 cm^{-1} (amide II), 1269 cm^{-1} (amide III), and at 893 cm^{-1}(skeletal vibration) are attributed to the α-helix structure. The peak at 660 cm^{-1} (amide V) comes from the random coil structure.

The spectral region between 1200 cm^{-1} and 1300 cm^{-1} has been selected to show change in amide III mode during powder processing, as this region is highly sensitive to conformational changes. When comparing scans a′ and b′ in Figure 2(a), it is clear that the sharpness of the shoulder at 1222 cm^{-1} increases after intensive degumming of eri silk indicating an increase in β-sheet content.[45,51] It was reported earlier that a strong 1222 cm^{-1} peak appeared when $(Ala)_n$ α helical fibers were stretched to form the β-sheet structure.[52] Similarly, the

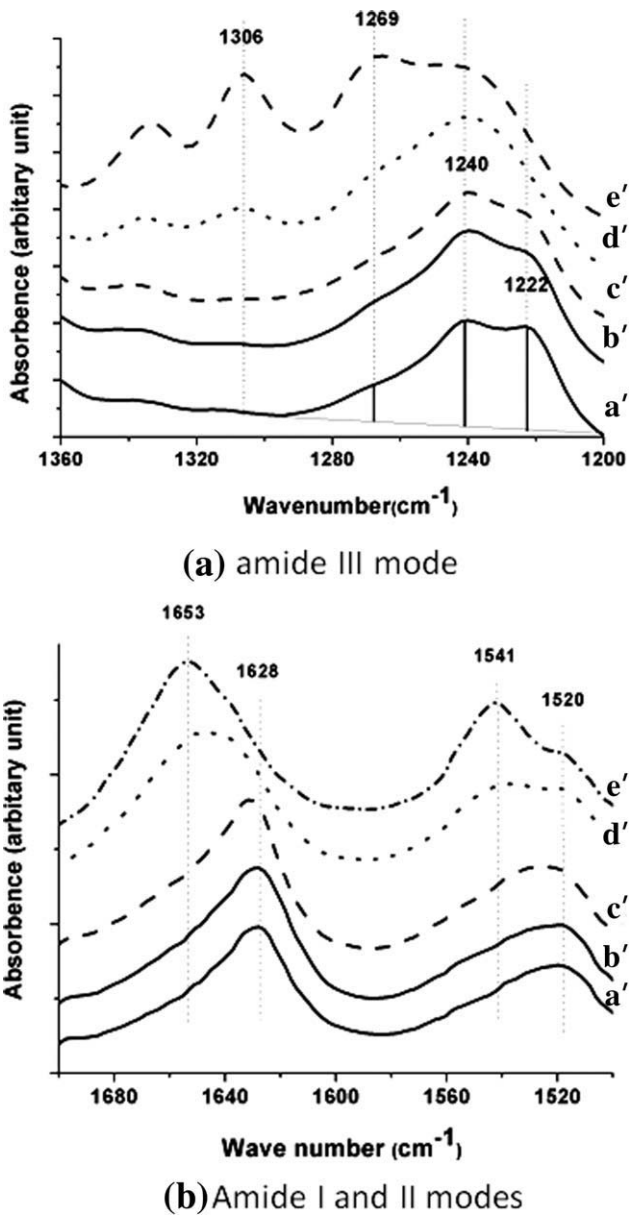

Figure 2 FTIR results of eri silk materials. (a′) Intensively degummed fiber, (b′) normal degummed fiber, (c′) 12 h wet milled powder, (d′) 8 h dry milled powder, and (e′) regenerated film.

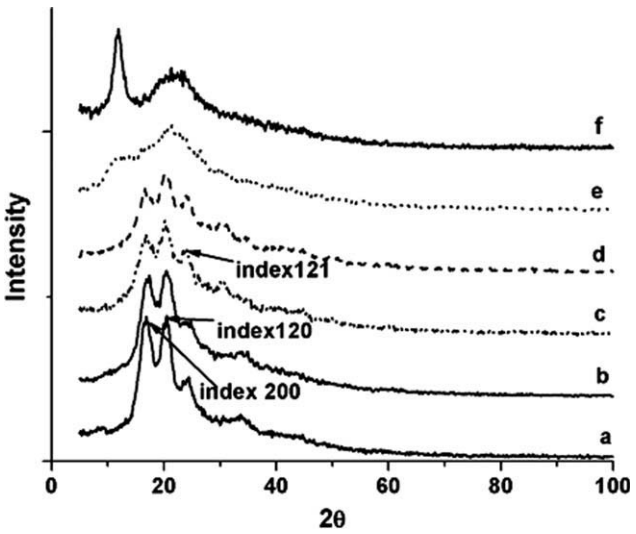

Figure 3 Wide angle X-ray diffraction spectra of eri silk materials. (a) Intensively degummed fiber, (b) normally degummed fiber, (c) 3 h wet milled powder, (d) 12 h wet milled powder, (e) 8 h dry milled powder, and (f) regenerated film.

strengthening of the β-sheet of *A. pernyi* silk upon enzymatic treatment and the corresponding increase in intensity of 1222 cm^{-1} peak was also reported.[45] It can also be seen from Figure 3 that sharp peaks characteristics of β-sheet appear after intensive degumming during WAXS (WAXS results are discussed subsequently) along with the 1222 cm^{-1} peak in FTIR scans [Fig. 2(a)] confirming an increase in β-sheet.

Scans b′ and c′ in Figure 2 are almost identical, suggesting that no conformational change occurred after 12 h wet milling compared with normal degummed fiber material. It has been noted that scans after air jet milling are similar to those obtained after attritor milling (results not shown), confirming again that no structural changes occurred during air jet milling. However, in the case of dry milled powder (scan d), the peaks at 1269 cm^{-1} and 1306 cm^{-1} started to emerge and the shoulder at 1222 cm^{-1} disappeared, indicating that mechanical forces during dry milling contributed to the significant changes in the secondary structure. Such changes are possible when intermolecular forces were ruptured and β structure was significantly lost. The scan e′ of regenerated fibroin film in Figure 2(a) shows that the peak due to the α-helix appears prominently at 1269 cm^{-1} along with another peak at 1306 cm^{-1}. The peak at 1269 cm^{-1} is higher than 1240 cm^{-1}. These results indicate dominance of α-helix in the film. The regenerated film could be dissolved in water instantly, which also confirms the lack of β structure. In addition to amide III, the spectra of amide I and II modes in Figure 2(b) also suggest that the FTIR pattern of dry milled powder looks more like a typical amorphous film (scan e′). There are some peak shifts after wet milling, albeit marginal. Unlike amide III mode, the increase in β-sheet component after intensive degumming cannot be identified in this spectral range.

Silk fibers were classified into different groups by Warwicker[53] according to WAXS patterns. The Saturniid family, which includes eri silk, falls under Group 3(a) of the classification for β crystal,[53] which has two prominent peaks at 2θ positions of 16.54° (index 200) and 20.40° (index 120) and a moderate peak at 24.3° (index 121) corresponding to crystalline plane spacings of 5.30 Å, 4.32 Å, and 3.67 Å, respectively. The WAXS spectra in Figure 3 show the presence of these peaks (scans a–d) for fibers and wet milled powders. The peaks of the intensively degummed fiber (scan a) are sharper than the normal degummed fiber (scan b). This agrees with the FTIR results (Fig. 2) and confirms that the crystallinity increases after intensive degumming. Unlike FTIR spectra, the WAXS results (Fig. 3) suggest marked changes in the diffraction pattern after wet milling. When comparing scans c and d with scan b, it is obvious that the height of the overall pattern is reduced with an increase in width along with the distinct drop in relative intensity between 16.5° and 20.4° peaks. The peak at 24.3° also appears to be sharper after wet milling. However, as the spectra are complicated with some peaks overlapping each other, it is difficult to predict whether the intensity of the area under the peak 24.3° actually increases. The WAXS results reveal that though the conformation remains as the extended β-sheet, which was also indicated by the FTIR scans, wet milling resulted in some structural disorder. The 2θ peak at 16.84° is for the index 200 plane, and normal of the plane lies in the direction of the side chain of the amino acid residues.[46,53] Therefore, these changes indicate rupture of intermolecular forces, such as van der Waals or other physical forces operating in that direction. The structural strength in the other two directions comes primarily from the hydrogen bond and protein backbone which could offer more resistance to the milling forces. In the case of dry milling, the peaks associated with the β-sheet completely disappeared (scan e of Fig. 3), which agrees with the FTIR result for the dry milled powder. The damage from dry milling can be attributed to the heat generated during milling, which cannot be practically avoided.[19] In regenerated film (scan f of Fig. 3), the peaks at 11.9° and 22° correspond to crystal spacing 7.4 Å and 4.03 Å corresponding to an α helical structure.[29,30,48,54]

The net crystalline β-sheet peak areas for different materials are determined by superimposing the WAXS pattern of the amorphous film over the pattern of respective material. Although there are approximations involved in the measurement, the peak area is used to compare materials instead of subtracting the amorphous background to calculate percentage

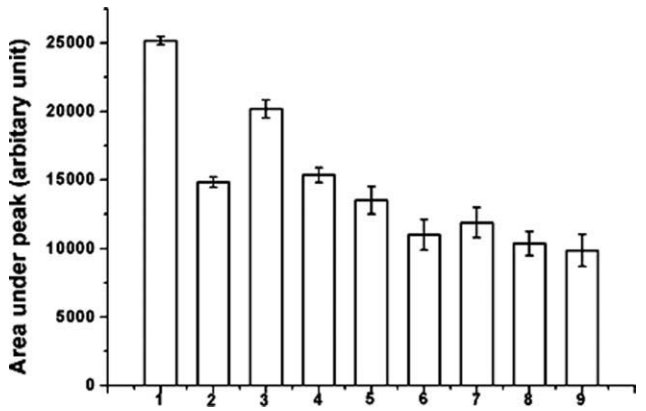

Figure 4 Area (mean ± SD) of β-sheet in eri silk materials. 1, Intensively degummed fiber; 2, 3 h wet milled after intensive degumming; 3, normally degummed fiber; 4–9, normally degummed powders (4, 3 h wet milled; 5, 6 h wet milled; 6, 12 h wet milled; 7, 3 h wet milled followed by air jet milling; 8, 6 h wet milled followed by air jet milling; 9, 12 h wet milled followed by air jet milling).

β-sheet crystallinity, as it is difficult to isolate the random coil scattering from the ordered α-helix scattering in the regenerated material. The average of four scans was used for calculating β-sheet fraction. The results in Figure 4 show that the area increases by about 25% after intensive degumming as compared with normal degumming. Irrespective of the degumming methods used, there is a gradual decrease in peak area as milling time increases. The normal degummed fibers were crushed into ultrafine powder with a volume distribution median particle size around 8 μm and 0.8 μm from 3 and 12 h wet milling, respectively, whereas the air jet milling reduced spray dried particle aggregates to generate individual sub-micron silk particles.[19] Apart from the attritor milling, the air jet milling also affects crystallinity, though the change from the process is relatively small as seen in Figure 4. In spite of the presence of intense mechanical energy during air jet milling, the process does not generate heat, and hence, it is suitable for heat sensitive materials, such as silk. Although the sharpness of WAXS peaks reduced after air jet milling, the particles remained stable and insoluble in water even when the particle size was reduced to the sub-micron level. However, the air jet milling is not suitable for direct milling of fibers unless intensive degumming treatment is used.[19] The SDS-PAGE, FTIR, and WAXS results demonstrate that wet milling with the attritor followed by air jet milling resulted in less degraded and more crystalline ultrafine silk particles than dry milling.

Transition of secondary structure in silk solution

When silk fibroin aqueous solutions were dialyzed, solutions from the intensively degummed fibers and dry milled powder formed hydrogel in 3–6 h. On the other hand, solution from wet milled powders could be dialyzed completely, but the dialyzed transparent aqueous solutions turned milky within 2–4 days when stored at 20°C as gelling started. As the milling hours increased, time to gel declined. Notably, the control degummed eri fiber and normal degummed mulberry silk fiber dialyzed solutions for which degradation was less according to SDS-PAGE results, could be stored at 20°C up to about three weeks, whereas the normal degummed eri dialyzed solution turned milky in about 1 week. Gelling in silk occurs due to the formation of β crystals.[9,55] In the case of synthetic polymers, it is well-established that crystallization is rapid with a decrease in molecular weight due to increased mobility of chains.[56] Although it is difficult to directly correlate β-sheet formation with a decrease in molecular weight due to the wide molecular weight distribution of silk after degumming, the results indicate that a sharp reduction of molecular weight helped faster β-sheet formation.

To study the conformational transition to β-sheet during storage of dialyzed aqueous silk samples from fiber and powder, the dialyzed solutions kept at 20°C for different times were used to cast films. To avoid β-sheet formation during film formation, the casting was carried out at 4°C. The films were then analyzed using FTIR and their results are presented in Figure 5. As seen from the scans a and b in Figure 5, the films obtained from normally degummed fiber show prominent α-helix structure

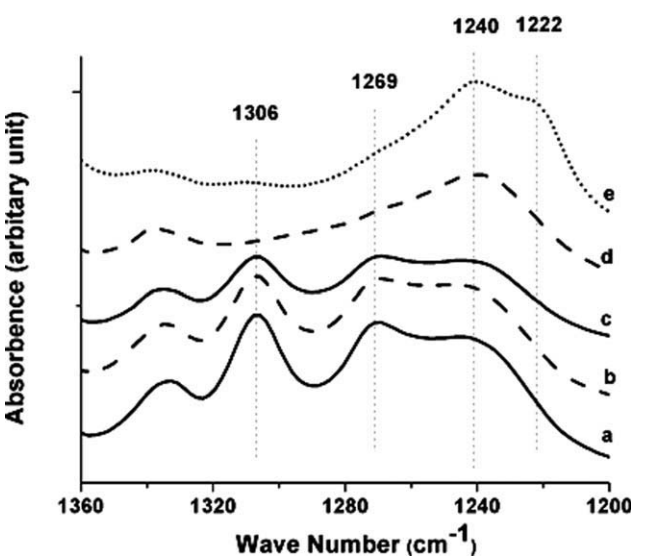

Figure 5 FTIR spectra (amide III mode) of films and dried gel from normally degummed eri silk. (a) From fiber, liquid without storage; (b) from fiber, liquid stored for 5 days; (c) from 12 h milled powder, liquid without storage; (d) from 12 h milled powder, liquid stored for 6 h; (e) from 12 h milled powder, liquid gelled during storage for 12 h.

characterized by the peak at 1269 cm^{-1}. These films were readily soluble in water. Scan c also shows similar characteristic. However, the α-helix peaks in scans a, b, and c disappeared after 6 h storage at 20°C as reflected in scan d in Figure 5. After storing for 12 h, the gelling of solution from the powder was so intense that no films formed because of structural transition to β-sheet as confirmed by the appearance of shoulder peak at 1222 cm^{-1} in the scan e in Figure 5. The scan e is quite similar to the starting material of the film, i.e., the 12 h milled powder shown in Figure 2 (scan c′). No FTIR results for films from intensive degumming and dry milled powder are available as these materials could not be dialyzed properly due to the formation of gels. The instant gelling of solution from highly degraded intensively degummed eri silk fiber suggests that the poor storage stability of the silk solution from powder was caused by molecular weight reduction, but not due to any attributes from milling, though synthetic polymers have a tendency to form free radicals and cross link structures during milling.[44] The results in Figure 5 further support that the molecular weight reduction is responsible for the increased rate of structural transition to form β crystals in the processed silk. It is also clear that the increase in crystallinity observed after intensive degumming according to FTIR and WAXS results is due to the reduction in molecular weight in the solid phase. This also happened during acid hydrolysis as reported by Bhat and Nadiger,[46] though no explanation was provided for such behavior. The increased milling rate of silk after intensive degumming[19] was helped by increase in brittleness due to higher crystallinity along with a reduction in molecular weight. The preliminary results provided some insight into the interrelationship between silk degradation and kinetics of β-sheet formation.

CONCLUSIONS

Alkali hydrolysis during silk degumming and forces during mechanical milling are responsible for lowering the molecular weight of silk particles. This reduction in molecular weight in turn reduces fiber strength, which helps silk milling. The changes in molecular weight and secondary structure from wet milling of normally degummed silk are moderate. The conformation of crystal forming domain was largely retained after wet milling though the WAXS peaks were reduced due to crystal order defects in the direction of side chains caused by the milling forces. During prolonged dry milling of silk, the molecular weight is drastically reduced and regular β-sheet structure is severely damaged. The structural transition of silk solution prepared from fiber and powder was highly influenced by the molecular weight.

We thank Dr. David Knight of Oxford Biomaterials for his advice on dialysis of eri silk and other valuable suggestions.

References

1. Minoura, N.; Aiba, S.-I.; Higuchi, M.; Gotoh, Y.; Tsukada, M.; Imai, Y. Biochem Biophys Res Commun 1995, 208, 511.
2. Tsubouchi, K.; Ninagawa, T. Jpn. Pat. JP 11104228 (1999).
3. Tsubouchi, K. Jpn. Pat. JP 2004123683 (2004).
4. Wang, Y.; Kim, H.-J.; Vunjak-Novakovic, G.; Kaplan, D. L. Biomaterials 2006, 27, 6064.
5. Hakimi, O.; Knight, D. P.; Vollrath, F.; Vadgama, P. Compos B 2007, 38, 324.
6. Vepari, C.; Kaplan, D. L. Prog Polym Sci 2007, 32, 991.
7. Dal Pra, I.; Freddi, G.; Minic, J.; Chiarini, A.; Armato, U. Biomaterials 2005, 26, 1987.
8. Jin, H.-J.; Chen, J.; Karageorgiou, V.; Altman, G. H.; Kaplan, D. L. Biomaterials 2004, 25, 1039.
9. Kim, U.-J.; Park, J.; Li, C.; Jin, H.-J.; Valluzzi, R.; Kaplan, D. L. Biomacromolecules 2004, 5, 786.
10. Fini, M.; Motta, A.; Torricelli, P.; Giavaresi, G.; Nicoli Aldini, N.; Tschon, M.; Giardino, R.; Migliaresi, C. Biomaterials 2005, 26, 3527.
11. Motta, A.; Migliaresi, C.; Faccioni, F.; Torricelli, P.; Fini, M.; Giardino, R. J Biomater Sci Polym Ed 2004, 15, 851.
12. Yasushi, T. Biomacromolecules 2005, 6, 3100.
13. Yoshimizu, H.; Asakura, T. J Appl Polym Sci 1990, 40, 127.
14. Amnat, J.; Yutaka, T.; Tanaka, H. Appl Microbiol Biotechnol 2006, 72, 726.
15. Zhang, Y.-Q. Biotechnol Adv 1998, 16, 961.
16. Wang, X.; Wenk, E.; Matsumoto, A.; Meinel, L.; Li, C.; Kaplan, D. L. J Controlled Release 2007, 117, 360.
17. Yeo, J.-H.; Lee, K.-G.; Lee, Y.-W.; Kim, S. Y. Eur Polym J 2003, 39, 1195.
18. Ha, S.-W.; Gracz, H. S.; Tonelli, A. E.; Hudson, S. M. Biomacromolecules 2005, 6, 2563.
19. Rajkhowa, R.; Wang, L.; Kanwar, J.; Wang, X. Powder Technol 2009, 191, 155.
20. Rajkhowa, R.; Wang, L.; Wang, X. Powder Technol 2008, 185, 87.
21. Dharmaprakash, M. S.; Rajkhowa, R.; Naik, R.; Huraeu, S.; Wang, L.; Smith, S. V. In Seventh International Conference on Nuclear and Radiochemistry; Budapest, Hungary, August, 2008.
22. Rajkhowa, R.; Gil, E. S.; Mieszawska, A.; Panilaitis, B.; Keiji, N.; Kludge, J. A.; Wang, L.; Wang, X.; Kanwar, J.; Kaplan, D. In 3rd Indo-Australian Conference on Biomaterials, Implants, Tissue Engineering and Regenerative Medicine; Sydney, 2009.
23. Zhang, Y.-Q.; Wei-De, S.; Ru-Li, X.; Zhuge, L.-J.; Gao, W.-J.; Wang, W.-B. J Nanopart Res 2007, 9, 885.
24. Wang, Q.; Jizhuang, C.; Huang, J.; Xu, X. Polym Eng Sci 1997, 37, 1091.
25. Molina-Boisseau, S.; Bolay, N. L. Powder Technol 2002, 128, 99.
26. Liang, S. B.; Hu, D. P.; Zhu, C.; Yu, A. B. Chem Eng Technol 2002, 25, 401.
27. Iridag, Y.; Kazanc, M. J Appl Polym Sci 2006, 100, 4260.
28. Yamada, H.; Nakao, H.; Takasu, Y.; Tsubouchi, K. Mater Sci Eng C 2001, 14, 41.
29. Tao, W.; Li, M.; Zhao, C. Int J Biol Macromol 2007, 40, 472.
30. Tsukada, M.; Freddi, G.; Gotoh, Y.; Kasai, N. J Polym Sci Part B: Polym Phys 1994, 32, 1407.

31. Zuo, B.; Dai, L.; Wu, Z. J Mater Sci 2006, 41, 3357.
32. Tsubouchi, K.; Nakao, H.; Igarashi, Y.; Takasu, Y.; Yamada, H. J Insect Biotechnol Sericology 2003, 72, 65.
33. Wang, X.; Wenk, E.; Hu, X.; Cascardo, G. R.; Lorenz, M.; Wang, X.; Li, C.; Merkle, H.; Kaplan, D. L. Biomaterials 2007, 28, 4161.
34. Hofmann, S.; Wong Po Foo, C. T.; Rossetti, F.; Textor, M.; Vunjak-Novakovic, G.; Kaplan, D. L.; Merkle, H. P.; Meinel, L. J Controlled Release 2006, 111, 219.
35. Wang, X.; Hu, X.; Daley, A.; Rabotyagova, O.; Cebe, P.; Kaplan, D. L. J Controlled Release 2007, 121, 190.
36. Baoqi Zuo, L. L.; Zhengyu, W.u J Appl Polym Sci 2007, 106, 53.
37. Kim, U.-J.; Park, J.; Joo Kim, H.; Wada, M.; Kaplan, D. L. Biomaterials 2005, 26, 2775.
38. Tsubouchi, K. U.S. Pat. 6440740 (2002).
39. Akiyama, D.; Hirabayashi, K. Polymer 1994, 35, 2355.
40. Hidefumi, T.; Kazushige, I.; Youichi, K.; Fumio, Y.; Tamikazu, K. Macromol Mater Eng 2000, 283, 126.
41. Xu, W.; Ke, G.; Peng, X. J Appl Polym Sci 2006, 101, 2967.
42. Rajkhowa, R.; Gupta, V. B.; Kothari, V. K. J Appl Polym Sci 2000, 77, 2418.
43. Inoue, S.-I.; Tsuda, H.; Tanaka, T.; Kobayashi, M.; Magoshi, Y.; Magoshi, J. Nano Lett 2003, 3, 1329.
44. Smith, A. P.; Shay, J. S.; Spontak, R. J.; Balik, C. M.; Ade, H.; Smith, S. D.; Koch, C. C. Polymer 2000, 41, 6271.
45. Taddei, P.; Arai, T.; Boschi, A.; Monti, P.; Tsukada, M.; Freddi, G. Biomacromolecules 2006, 7, 259.
46. Bhat, N. V.; Nadiger, G. S. J Appl Polym Sci 1980, 25, 921.
47. Sen, K.; Babu, M. J Appl Polym Sci 2004, 92, 1098.
48. Freddi, G.; Monti, P.; Nagura, M.; Gotoh, Y.; Tsukada, M. J Polym Sci Part B: Polym Phys 1997, 35, 841.
49. Kweon, H. Y.; Park, H. Y. J Appl Polym Sci 1999, 73, 2887.
50. Freddi, G.; Tsukada, M.; Bertta, S. J Appl Polym Sci 1999, 71, 1563.
51. Moore, W. H.; Krimm, S. Biopolymers 1976, 15, 2465.
52. Frushour, B. G.; Koenig, J. L. Biopolymers 1974, 13, 455.
53. Warwicker, J. O. J Mol Biol 1960, 2, 350.
54. Tsukada, M.; Freddi, G.; Monti, P.; Bertoluzza, A.; Kasai, N. J Polym Sci Part B: Polym Phys 1995, 33, 1995.
55. Wang, X.; Kludge, J. A.; Leisk, G. G.; Kaplan, D. L. Biomaterials 2008, 29, 1051.
56. Mandelkern, L. Biophys Chem 2004, 112, 109.